ARC Joint: Anthropomorphic Rolling Contact Joint With Kinematically Variable Torsional Stiffness

Seungyeon Kim, Eunho Sung, and Jaeheung Park

***Abstract*—As compliant joints not only compensate for the lack of actuated degrees of freedom of an under-actuated system and improve grasp stability but also prevent system failure from unexpected contacts, various types of compliant joints have been applied to end-effectors. Although joint compliance increases the success rate of power grasping, when the finger wraps around large objects, it can reduce the grasping success rate in pinch gripping when dealing with small objects using the fingertips. To overcome this drawback, we propose a novel rolling contact joint, *anthropomorphic rolling contact joint*, that mimicked the structures of the human finger joint, tongue-and-groove, and collateral ligaments. The anthropomorphic rolling contact joint can passively adjust the torsional stiffness according to the joint angle without additional weight and space. With the anthropomorphic rolling contact joint, flexing the fingers for pinch grasping increases torsional stiffness of the joints and improves grasping stability. In this study, the characteristics and performance of anthropomorphic rolling contact joints were experimentally analyzed by varying the tongue-and-groove shape. Furthermore, it was demonstrated that the three-finger gripper with high torsional stiffness stably grasps small objects in the pinch grasping posture. In addition, because it is easy to manufacture, an anthropomorphic rolling contact joint has advantages in terms of maintenance.**

***Index Terms*—Compliant joints and mechanisms, mechanism design.**

I. Introduction

As ROBOTICS has advanced, people encounter an increasing number of robots in various fields of daily life. Unlike gigantic industrial robots that are used in a space separated from humans, small manipulators have recently been developed for multiple tasks and directly cooperating with people. However, what the manipulator can perform is determined by what the end-effector can do because it is the gateway that directly interacts with the surrounding environment or objects. Unlike various commercially available manipulators that are similar in shape and specification with six or seven degrees of freedom, most end-effectors are designed based on a task to be performed. Therefore, even if a general-purpose manipulator is used, only the work targeted by the end-effector can be performed.

To conduct various tasks in human-centered environments, an end-effector with the performance, size, and weight of a human hand can be considered ideal. Although many studies have developed end-effectors, to overcome these lack of performance, human-hand-level end-effectors have not yet been developed [1].

Recently, various end-effectors using soft materials, such as silicone, have been studied. The flexibility of the material enables the gripper to interact with the surrounding environment and objects actively, and this adaptiveness makes it possible to stably grasp various objects by compensating for the low degrees of freedom or lack of sensors. Compared with conventional rigid grippers, which are capable of adaptive grasping only in the joint driving direction, soft grippers can grasp objects more stably with passive shape deformation [2].

Manti et al. designed soft grippers with three fingers using two types of silicone [3]. This soft gripper uses only one tendon-driven actuator, but it shows that stable grasping postures are accomplished regardless of the shape of the objects using the compliance of silicone and the adaptive mechanism of each finger. Furthermore, studies have been conducted to grasp objects using the fingertips of soft grippers with multiple actuators for one finger. Zhou et al. showed that a three-finger soft gripper with six degrees of freedom can handle a small object using the fingertips, in which cylindrical bumps were applied [4]. Teeple et al. designed a soft finger comprising two parts and experimentally analyzed the success rates of power grasping and pinch grasping based on the ratio of the two parts [5]. However, precise control of soft grippers compared to grippers consisting of rigid materials (plastic, aluminum, steel, etc.) still remains a big challenge.

To compensate for the shortcoming of soft grippers, various hybrid-type grippers have been developed, whose bones consist of rigid materials but joints consist of soft material, such as urethane joints and rolling contact joints with elastic ligaments [6], [7], [8], [9].

However, the fact that each joint can adapt to external forces implies that the fingertip position cannot be maintained at the desired position when contact occurs on the end-effectors. As shown in Fig. 1, in power grasping, the surfaces of each phalange are in close contact with the surface of an object, which improves the grasping stability. However, when grasping using the

This work was supported by the Institute of Information & Communications Technology Planning & Evaluation (IITP) funded by the Korea Government (MSIT) under Grant 2021-0-00896.*(Corresponding author: Jaeheung Park.)*

Seungyeon Kim and Eunho Sung are with the DYROS Lab, Graduate School of Convergence Science and Technology, Seoul National University, Seoul 08826, Republic of Korea (e-mail: ksy0711@snu.ac.kr; eunho526@snu.ac.kr).

Jaeheung Park is with the DYROS Lab, Graduate School of Convergence Science and Technology, Seoul National University, Seoul 08826, Republic of Korea, and also with the Advanced Institutes of Convergence Technology(AICT), Suwon 16229, Republic of Korea (e-mail: park73@snu.ac.kr).

This letter has supplementary downloadable material available at https://doi.org/10.1109/LRA.2023.3243439, provided by the authors.

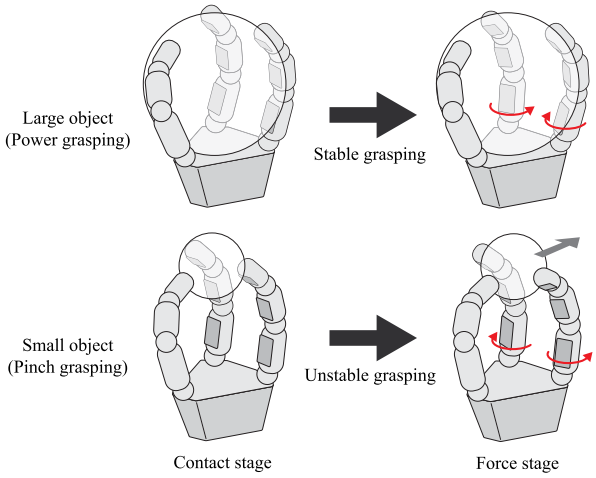

Fig. 1. Influence of joint compliance when grasping a large object and small object. The small object can be ejected from the fingertips due to the changes in fingertip position.

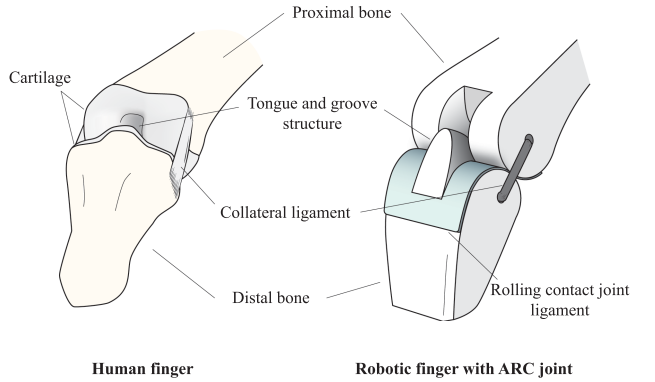

Fig. 2. Comparison between components of human finger joint and ARC joint. The structure of the ARC joint was inspired by contact surface shapes and collateral ligament of the finger joints. The left shows distal interphalangeal joint of human finger, and the right shows the proposed ARC joint.

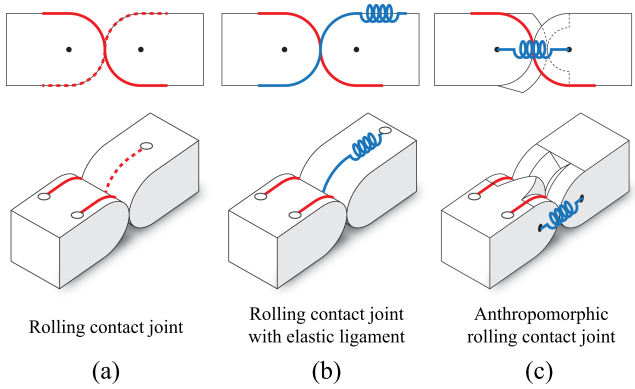

Fig. 3. Diagrammatic comparison between Rolling Contact joints, (a) Conventional rolling contact joint, (b) Rolling contact joint with extensible ligament, (c) Anthropomorphic rolling contact joint. Red lines represent in-extensible tendon, and blue ones represent extensible tendon.

fingertip, such as pinch grasping, the objects are ejected between the fingers, and the grasping success rate decreases because of changes in the fingertip position. Various studies related to adjusting joint compliance have been conducted, but the mechanisms require additional size and weight of the end-effectors.

Human joints actively control the stiffness of a joint by using ligaments constituting the joint and surrounding muscles, and if joint stiffness can be actively adjusted, the aforementioned limitations can be improved. Zhu et al. analyzed the joint structure of human fingers and proposed a highly biomimetic joint that realize musculoskeletal characteristics. However, because of complex structure of the joint that is difficult to manufacture and customize, the highly biomimetic joint is applicable only to limited robotic systems like robotic hand [10], [11].

In this study, we propose a novel compliant rolling contact joint, an anthropomorphic rolling contact joint (ARC joint), whose torsional stiffness passively increases according to the joint angle to realize low joint stiffness in power grasping and high joint stiffness in pinch grasping without additional weight and size. The ARC joint mimics the structures of the human finger joint, tongue-and-groove, and collateral ligaments, improving the structure of the existing rolling contact joint, and Fig. 2 shows a comparison between the human finger joint and ARC joint.

The remainder of this letter is organized as follows. In Section II, we introduce related studies on rolling contact joints. Section III describes the detailed design structure, including the differences between the previous rolling contact joints and ARC joint. The experimental results of the joint stiffness of the ARC joint are presented in Section IV. In Section V, the functionality of the ARC joint is experimentally demonstrated by applying the ARC joint to two different three-finger robotic grippers. Finally, Section VI concludes the paper.

II. Related Works: Rolling Contact Joint

According to a patent proposed by Hillberry, the basic structure of the rolling contact joint is illustrated in Fig. 3(a). Two ligaments intersect and connect to each bone, and because of the constraint that the length of the ligaments is maintained, the surfaces of both bones can roll without slipping [12]. Compared with the revolute pin joint, the rolling contact joint has the following advantages. First, it can withstand a stronger force than to a pin joint in a compact structure [13]. This is because the ligament supports the tensile force and the bone supports the compressive force. Second, it is possible to manufacture them inexpensively because expensive parts, such as bearings, are not required. Third, it has a wide range of motion by avoiding self-collision compared to the pin joint. Because of these characteristics, the rolling-contact joint has been applied to various end-effectors, such as grippers and robotic hands, including an artificial implant joint [14], [15].

However, the rolling contact joint has limitations. First, the performance of the joint is guaranteed only when the two ligaments are fixed exactly in the correct position on the two bones. If the length is slightly longer, a gap occurs between the two bodies, such as the backlash of gears, and if the length is short, assembly becomes impossible. Second, it cannot compensate for any ligament stretching that occurs during the actual operations. If the ligament is stretched owing to external impact or repeated

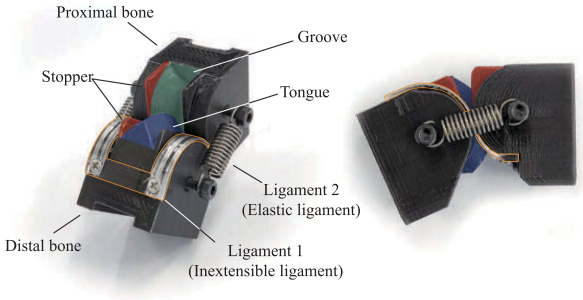

Fig. 4. Details of manufactured ARC joint. Left figure shows component name of ARC joint in perspective view, and right figure shows lateral view of ARC joint.

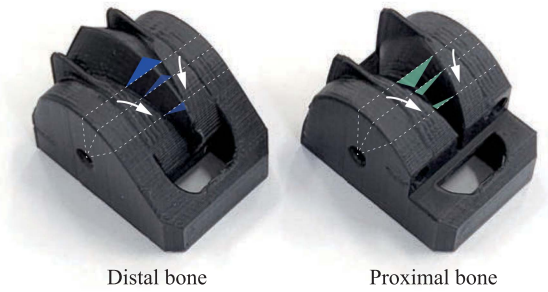

Fig. 5. Example shape of tongue-and-groove. To reduce the number of required ligaments, the shape should be narrowed in the direction of the arrow.

use, the aforementioned problem occurs. However, because the ligaments of the rolling contact joint are installed between the bones and cross each other, replacing the ligaments requires more effort than repairing the pin joint.

To complement the limitations, various types of rolling contact joints with compliant material have been studied [7], [9], [16]. Kim et al. proposed a rolling contact joint in which an elastic element is applied to one of the two ligaments, as shown in Fig. 3(b) [6]. With this compliant ligament, the rolling contact joint can not only absorb the impact force acting on the finger and prevent damage, but also compensate for the elongation and manufacturing error of ligaments. By designing different pulley radii for the proximal and distal bones of the elastic ligament, a passive extension force without additional mechanisms was implemented. However, the joint compliance caused by the application of an elastic ligament to the rolling contact joint has not been analyzed, and there are no previous studies related to effect on object grasping stability.

III. Anthropomorphic Rolling Contact Joint

In this section, the structure of the ARC joint and its fundamental working principle are introduced. Next, the advantages of the ARC joint are discussed.

A. Fundamental Components of Arc Joint

The ARC joint mimics the two components in human finger joints, the tongue-and-groove mechanism, and collateral ligaments; these are known to improve joint stability [17], [18]. Fig. 4 shows the detailed structure of the ARC joint, and we overlaid the colors on each component for better visibility. Similar to human joints, grooves (green) and tongue (blue) are designed on the contact surface of the proximal and distal bones, and two types of ligaments are used to constrain these two bodies. These two ligaments have opposing properties. Ligament 1 (orange) is located between these two bodies and prevents slipping on the surface of each bone and should be manufactured using an inelastic material. Conversely, Ligament 2 should have elasticity for joint compliance and is located beside the two bones, similar to collateral ligaments in the human joint finger (Fig. 2). Unlike the elastic ligament of previous rolling contact joints (Fig. 3(b)), Ligament 2 of the ARC joint can only compensate for the short Ligament 1, and elongation of Ligament 1 causes backlash. In addition, a stopper was placed beside the tongue and groove to prevent hyperextension.

In this study, we used commercial springs as Ligament 2; however, various elastic materials can be applied. When torsional rotation occurs in the ARC joint, the distance between the centers of the two bodies increases, and Ligament 2 exerts a restoration force owing to the interference of the tongue-and-groove structure. Therefore, the elastic modulus of Ligament 2 should be determined by considering the purpose of the joint.

Fig. 5 shows an example of the shape of the tongue and groove. One of the most important design features of the ARC joint is that the shape of the tongue and groove of the ARC joint should be narrowed in the direction of the arrow (white arrow in Fig. 5) to reduce the number of required ligaments located between the bodies. Without this characteristic, the joint could not resist the $+y$ displacement of the distal bone (Table I). The interference between the wide tongue and narrow groove elongates the collateral ligament when a $+y$ displacement occurs. In the case of humans, there is a slight difference between the shape of the tongue and groove but the same shape was applied in this study [19].

The linear and angular stiffnesses along each direction were determined differently from those of the conventional rolling contact joint. The components that determine the stiffness in each direction are shown in Table I. The relative displacements of the distal bone are expressed in the coordinates of the distal bone, O_d. Most stiffnesses are determined by the elastic coefficient of Ligament 2 and the shapes of the tongue and groove. However, the linear stiffness along $-x$ and $-y$ is determined by the material properties of bones and Ligament 1, respectively. In most cases, these are much larger than the stiffnesses of the other directions. This is because the bones are made of a rigid material, and Ligament 1 has inextensible properties.

This difference between the stiffnesses in the positive and negative y-directions is the main reason why we selected the bone with a groove as the distal bone of the finger joint. In most object grasping situations, the forces acting perpendicular to the bottom surface of the bone ($+y$ direction) are reaction forces from the grasped object. Therefore, for firm grasping, the joint should resist the force that does not conform.

TABLE I
COMPONENTS THAT DETERMINE LINEAR/ANGULAR STIFFNESS ALONG EACH DIRECTION

	Direction of displacements of distal bone	Linear stiffness	Angular stiffness
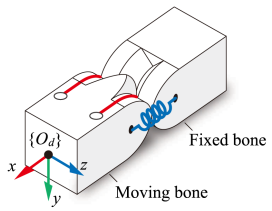	$+x$	Elastic coefficient of collateral ligaments	Elastic coefficient of collateral ligaments and shape of tongue and groove
	$-x$	Material property of bones	
	$+y$	Elastic coefficient of collateral ligaments and shape of tongue and groove	Elastic coefficient of collateral ligaments and *partially* shape of tongue and groove
	$-y$	Material property of ligament	
	$+z$	Elastic coefficient of collateral ligaments and shape of tongue and groove	Ideally zero stiffness
	$-z$		

One of the advantages of rolling contact joints is that the z-direction rotational stiffness and friction are zero because there is no slip between the surfaces. Ideally, the z-direction rotational stiffness of the ARC joint is also zero, but because of the slip between the surfaces of the tongue and groove friction occurs when the joint is rotated. Therefore, in applications where little friction is required and no lateral force or twist torque exists, the conventional rolling contact joint will be more suitable than the ARC joint. However, in applications that need to adapt to external forces in various directions, such as robotic fingers, the ARC joint has advantages.

B. Advantages of Arc Joint

The first advantage of the ARC joint is that its stability is improved. With the collateral ligament, stability against torsional twist, as described above, as well as stability against translation in the x, y, and z directions, and rotation in the y direction is significantly increased. These values can be modified by adjusting the shape parameters of the ARC joint, including elastic modulus of the collateral ligament and tongue-and-groove shape. In particular, it has the advantage of being able to express the desired characteristics according to design parameters, unlike previous studies that eliminated compliance in a specific direction by using a gear shape to overcome the problems of the existing rolling contact joint.

Second, the ARC joints have advantages in terms of manufacturing. The ARC joint can be reassembled after a complete disassembly, and the reduced number of ligaments that pass between the bones from two to one makes it easier to design and assemble. This is because, unlike other rolling contact joints that use knots or adhesives to fix ligaments to bones in the manufacturing process, ligaments of ARC joints can be fixed using screws and can be disassembled without damage. As a result, the use of ARC joint not only allows for easy maintenance but also significantly reduces the error in joint performance that can occur depending on the skill of the assembler.

IV. TORSIONAL STIFFNESS EVALUATION

A. Experimental Setup

Fig. 6 shows the experimental setup used to measure the torsional stiffness of the ARC joints at various angles of the joint. Using two actuators (ROBOTIS, XH430-W210-T), the torsional stiffness could be measured without human interference, after the test subject was installed. Actuator 1 changes the joint angle

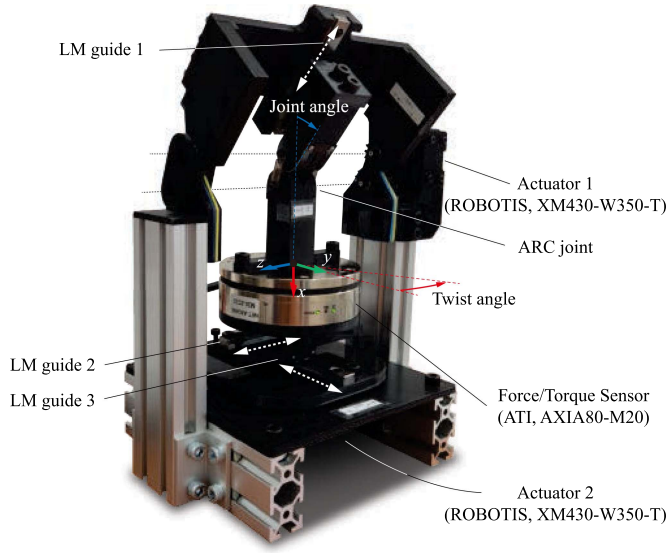

Fig. 6. Experimental setup to evaluate torsional stiffness ARC joints.

(q) of the ARC joint, and actuator 2 adjusts the twist angle (θ_{twist}) of the distal bone. The motion of each actuator is shown in Fig. 6 with blue and red arrows. A force/torque sensor (ATI Industrial Automation, AXIA80-M20) was installed between actuator 2 and the distal bone to measure torque in the vertical direction.

The twist movement of actuator 2 generates relative motion between the two bones. First, torsion causes interference between the tongue and groove structure, thereby increasing the distance between the two bones. The second relative motion is generated in the yz-plane in Fig. 6 because of Ligament 2. Depending on the rotational direction of the proximal bone, slack occurs on one side of Ligament 1 and a tensile force acts on the opposite side. Owing to the inextensible characteristic of Ligament 1, the rotational center of the proximal bone should be located on Ligament 1, not on the center of the bones. Considering the influence of these relative motions, three linear motion guides (LM guides) were installed in the experimental setup. The locations and movement directions of each LM guide are shown in Fig. 6.

B. Design and Manufacturing of Arc Joints

Fig. 7 shows the design parameters of the ARC joint, and Table II shows the dimensions of the ARC joints used in this

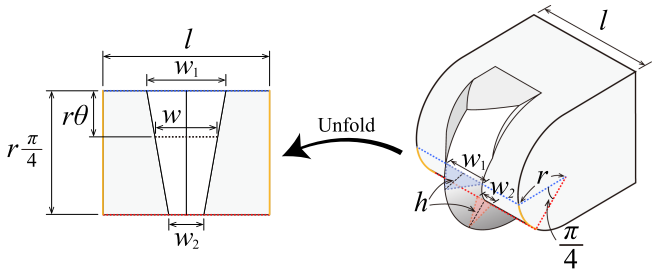

Fig. 7. ARC joint design parameters of proximal bones. In this study, the ARC joints had triangular tongue and groove shape with identical height. Left figure shows unfolded contact surface from $\theta = 0$ to $\theta = \pi/4$.

TABLE II
DIMENSIONS OF SIX ARC JOINTS WITH DIFFERENT TONGUE AND GROOVE SHAPES AND A JOINT WITHOUT TONGUE AND GROOVE SHAPE

Name	r	l	h	w_1	w_2
w7-6	10 mm	20 mm	4 mm	7 mm	6 mm
w7-5					5 mm
w7-4.5					4.5 mm
w7-4					4 mm
w7-3.5					3.5 mm
w7-3					3 mm
w0-0				0 mm	0 mm

experiment. The radius (r) of the contact surface was 10 mm and the width (l) of the two bones was 20 mm. Each dimension is determined by considering the size of the robotic fingers. In this study, we applied a triangular shape to evaluate the influence of different shape of tongue and groove mechanism. The height (h) and width (w_1) of the tongue and grooves at 0° were fixed at 4 mm and 7 mm, respectively. Six different ARC joints were manufactured with different w_2, widths at 90°, from 3 mm to 6 mm. The w value according to the angle was linearly interpolated using (1).

$$w(\theta) = w_1 + \frac{4\theta}{\pi}(w_2 - w_1) \tag{1}$$

To achieve manufacturing repeatability of the joint, the bones of the ARC joints and Ligament 1 were manufactured using an FDM-type 3D printer (Ultimaker S5) with tough polylactic acid (PLA). The ligament produced through 3D printing allows it to be combined in a more precise position than the conventional method using a string. The disadvantage of this method is that ligaments made of PLA are vulnerable to repeated flexion. To improve this problem while maintaining the simplicity of fabrication fiberglass tape was applied on both sides of the ligament. Two commercial springs were used for Ligament 2; the free length, spring coefficient, and initial tension were 18.1 mm, 0.99 N/mm, and 2.501 N, respectively.

C. Torsional Stiffness Change According to Joint Angle and Twist Angle

In this study, to evaluate the stiffness characteristics of the ARC joint, the torsional torque (τ_z) was measured by the force/torque sensor when twisted by θ_{twist} in both directions. The average torsional stiffness (S) was calculated by dividing the sum of the absolute values of the torques by the total amount of twist ($2 \cdot \theta_{twist}$), as shown in (2). The average torsional stiffness was estimated for various joint angles and twist angles using different ARC joints with the dimensions listed in Table II.

$$S = \frac{|\tau_{+x}| + |\tau_{-x}|}{2 \cdot \theta_{twist}} \tag{2}$$

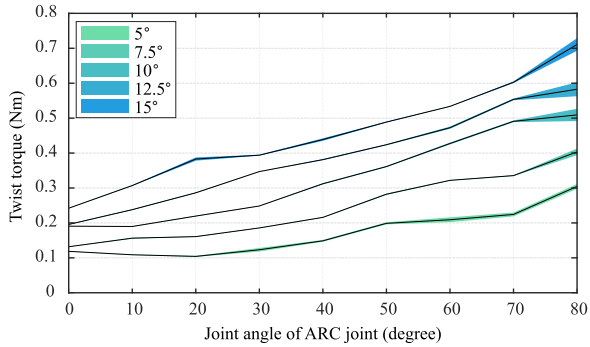

Fig. 8. Average twist torque of w7-3 under different twist angles.

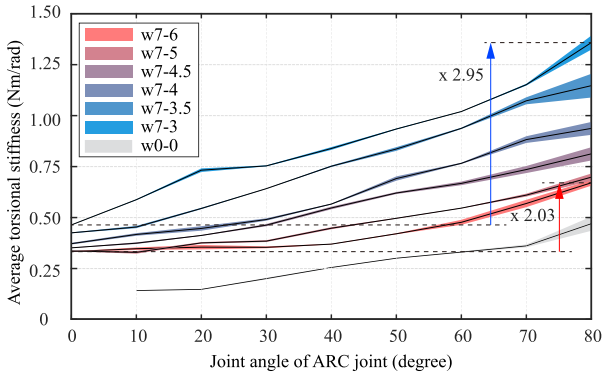

Fig. 9. Average torsional stiffness of ARC joint under 15° twist angle.

Fig. 8 shows the twist torques ($|\tau_{+x}| + |\tau_{-x}|$) of w7-3 ARC joint. Experiments were conducted from 0° to 80° at 10° intervals, and the twist angle varied from 5° to 15° at intervals of 2.5°. The measurements were repeated 5 times in all cases. The solid black lines represent the average of five measured values, and each colored area represents $\pm\sigma$ (standard deviation) from the normal value.

The average torsional torque increased as the twist angle increased for all joint angles. However, it can be observed that there was a difference in the amount of change depending on the joint angle. The twist torque increased most linearly at a joint angle of 40°, and it was observed that the linearity decreases significantly as the joint angle approaches 0° and 80°.

Fig. 9 shows the torsional characteristics of the six ARC joints with different tongue-and-groove shapes (Table II). The average torsional stiffness was measured in the same range of joint angles as those in the previous experiment. The experiments were conducted five times at a twist angle of 15° in all the cases. The solid line indicates the average value and the colored area indicates $\pm\sigma$ from the average.

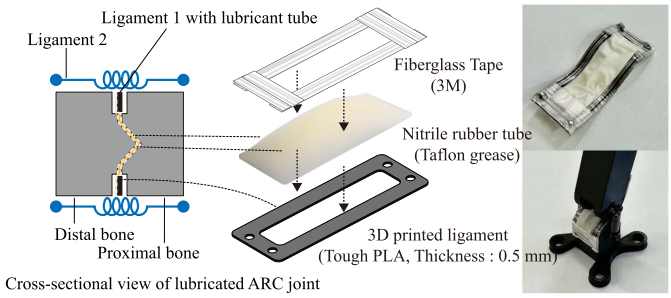

Fig. 10. Ligament 1 with lubrication structure. Left shows detail of Ligament 1, and right shows fabricated Ligament 1 and ARC joint with lubrication structure.

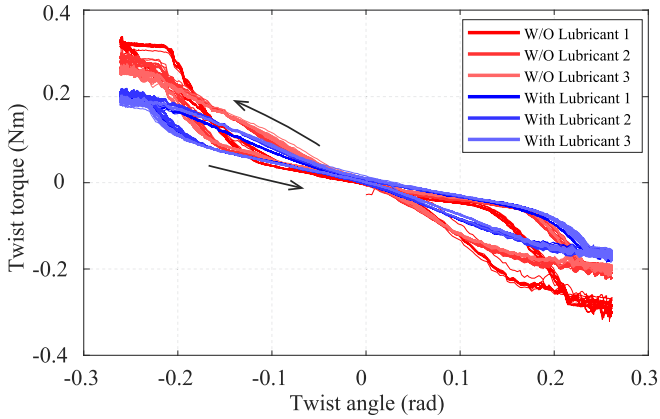

Fig. 11. Twist toque of six w7-3 ARC joints at 60° joint angle with/without lubrication structure according to twist angle.

In most cases, six different ARC joints had a tendency to increase torsional stiffness as the joint flexed, but in case of w7-6, the torsional stiffness from 0° to 40° was maintained. As w_2 decreased, the rate of change in torsional stiffness increased. Comparing the torsional stiffness at 0° and 80°, in the case of w7-3, it increased to 2.95 times (0.46 Nm/rad to 1.36 Nm/rad), while in the case of w7-6, it increased to 2.03 times (0.33 Nm/rad to 0.67 Nm/rad). Also, the results showed that ARC joints with a tongue and groove structure had a higher average torsional stiffness than W0-0 for all joint angles. When the joint angle was 80°, the average torsional stiffness of w7-6 and w7-3 were 1.43 and 2.89 times that of w0-0, 0.47 Nm/rad, respectively.

The results in Fig. 9 show that the torsional stiffness of the ARC joint is influenced not only by the instantaneous tongue-and-groove shape but also by the rate of shape change. Although the tongue and groove shapes of the six ARC joints used in the experiment were the identical at a joint angle of 0°, torsional stiffness increased as w_2 decreased. This is because the amount of interference between the two bones caused by torsion increased as $|\frac{\delta w}{\delta \theta}|$ increased.

D. Torsional Stiffness With Lubrication Structure

Unlike the rolling contact joint, the ARC joint generates friction between the tongue and the groove during joint flexion/extension and twisting, which cause abrasion and degrade joint performance. Fig. 10 shows Ligament 1 with a lubrication structure to reduce the friction between tongue and groove. A nitrile rubber tube containing teflon grease was combined with Ligament 1 using fiberglass tape. In this study, Ligament 1 manufactured by 3D printer using tough PLA, and fiberglass tape complements the durability of Ligament 1. The proposed lubrication structure was completely sealed so that the teflon grease was not lost during the joint motion.

Fig. 11 shows the twist torque of six w7-3 ARC joints according to the twist angle at 60° joint angle. Red lines represent the twist torque of three w7-3 ARC joints without lubrication structure, and blue lines represent that of three w7-3 ARC joints with lubrication structure. The experiment results showed that the ARC joint with the lubrication structure not only measured a smaller maximum twist torque than the ARC joint without the lubrication structure, but also showed small performance differences between individuals.

V. Grasping Performance Comparison of Grippers With Different Arc Joints

To verify the effect of the ARC joint on the grasping process, we fabricated two three-finger grippers with different tongue-and-groove shapes (w7-6 and w7-3) and observed their grasping stability. When the ARC joint, whose stiffness increases according to the joint angle, is applied to the robotic finger, it is possible to stably pinch grasp a small object by utilizing high joint stiffness. Simultaneously, stable contact with an object or environment is feasible with stretched fingers in the early stage of grasping.

Fig. 12(a) shows a three-finger gripper with ARC joint, and Fig. 12(b) shows the structure of a single modular finger. The gripper consists of Finger 1, Finger 2, and Finger 3, facing each other. The distance between Finger 2 and Finger 3 was 52 mm considering the width of the modular finger (22 mm), and Finger 1 was located in the middle of Finger 2 and Finger 3. The force sensor (Optoforce, 3D force sensor) could be attached to the distal phlange of Finger 1 to measure the contact force while grasp objects. The total weight of the gripper was estimated at 291 g.

The three fingers were designed with the same structure except for the actuator. The finger consists of four links (metacarpal, proximal phalanx, middle phalanx, and distal phalanx) and metacarpal (MCP), proximal interphalangeal (PIP), and distal interphalangeal (DIP) joints. The three joints had the same structure as the ARC joint used in the previous experiment (Fig. 4). Three identical ARC joints were driven by an actuator using a tendon-driven mechanism. In free motion, all three joints were actuated identically owing to the two coupling ligaments. Because the actuating tendon was fixed to the middle phalanx, it enabled adaptive grasping by actuating the DIP and PIP joints even when contact occurred on the proximal phalanx. A silicone cover (Shore 40 A) was applied to the fingertips and palm of the gripper to improve grip stability.

Finger 2 and Finger 3 were actuated by XC330-M181-T from ROBOTIS, and Finger 1 was actuated by XC330-M288-T, which has a higher reduction ratio than XC330-M181-T. This is because Finger 1 must withstand the force of the two opposing

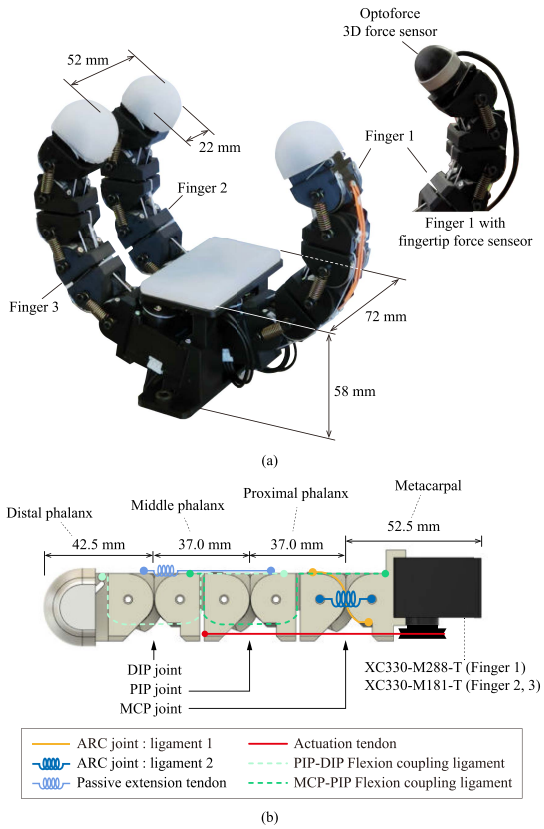

Fig. 12. Detail of gripper and modular finger, (a) Overall design of the three-finger gripper, (b) Design and ligaments of fully extended modular finger. Ligaments related with ARC joint are representatively illustrated on MCP joint.

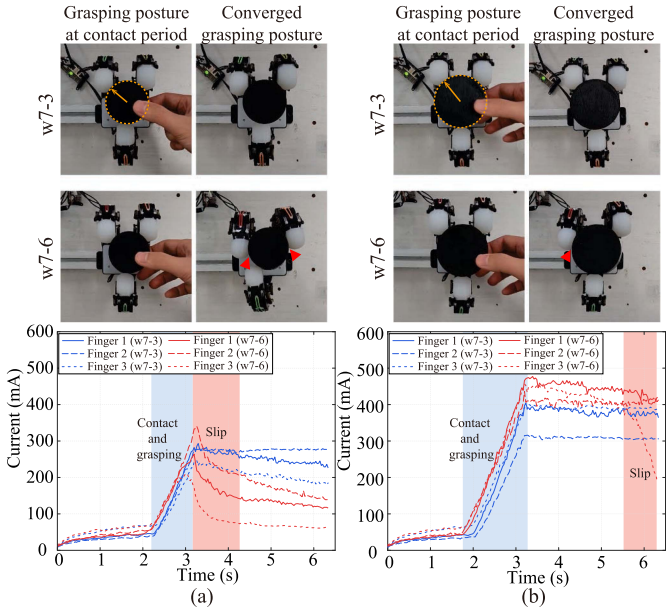

Fig. 13. Grasping postures (top view) and actuator currents of each finger during grasping a cylinder-shaped object with different diameters, (a) 50 mm diameter, (b) 60 mm diameter.

fingers in the process of grasping an object. The maximum fingertip force of finger 1 under MCP, PIP, and DIP joint 30 degrees was 2.2 N, and the maximum fingertip force of Finger 2 and 3, which have lower reduction ratio, under the same posture was 1.3 N. The maximum fingertip forces were estimated with 600 mA motor current.

Fig. 13 shows the results of the grasping experiment using two different grippers. For the experiment, cylinders with two different diameters of 50 mm (Fig. 13(a)), and 60 mm (Fig. 13(b)) were used. The above pictures show the grasping postures when contact between the object and the fingertip occurred and the final converged grasping postures in each case. The graphs below show the instantaneous current values of each finger during the object-grasping process. With the current graphs, the status of the fingertips could be analyzed because the currents were controlled to be proportional to the position error. In the process of grasping the object, the desired positions of the actuators were designed to flex the finger at a constant speed, which implies that if contact with an object occurs while flexing the finger, the position error and input current increase. Conversely, when a slip occurs between the object and the fingertip, the current value drops rapidly. In the graphs, blue lines represent the currents of the finger with the w7-3 ARC joints, and the red lines represent the currents of the finger with the w7-6 ARC joints. It was observed that the current value of the fingers gradually increased before contact occurred because the passive extension tendon extended as each finger flexed.

The smaller the radius, the more often slippage was observed. As the diameter of the object decreased, the direction of the reaction force (orange arrows in Fig. 13) transmitted from the object to the fingertips became more horizontal. Each finger can only control the vertical force, and the horizontal force is determined by the stiffness of the joint and the amount of deformation of the fingertip position. As the object becomes smaller, the joint angle at the contact period increases, which not only increases the joint stiffness, but also the reaction force in the horizontal direction. The horizontal component of the reaction force increases rapidly as the diameter of the object approaches the distance between Finger 2 and Finger 3 (30 mm), resulting in more fingertip position changes and slips.

In particular, in the process of grasping a cylinderical object with a diameter of 60 mm, it seemed that the initial object was stably gripped, but slippage occurred over time. This implies that even if the initial grasp is stable, the grasping easily becomes unstable, and the object can be dropped with a slight disturbance. The gripper with w7-3 ARC joints firmly grasped the objects with diameter 50 mm and 60 mm, and the current values of each finger showed that they maintained grasping forces without slippage.

To estimate the maximum grasping force of two grippers when grasp cylinder-shape objects, a force sensor (OPTOFORCE, 3D Force sensor) was attached to the fingertip of Finger 1 (Fig. 12(a)). The maximum grasping force was defined as the fingertip force at the moment when grasping became unstable due to slippage occurred. Fig. 12 shows the results of maximum grasping force that each gripper can apply to a cylinder-shaped object using box-plot, and the circle points show 50 repeated grasps for each case. When grasp 50 mm cylinder, the average

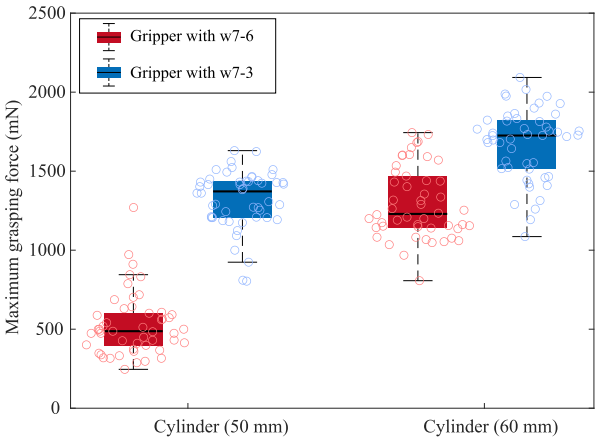

Fig. 14. Maximum grasping force of two grippers grasping cylinders with 50 mm and 60 mm diameters.

maximum grasp force of gripper with w7-6 and w7-3 were 526 mN and 1320 mN, respectively, and grasping 60 mm cylinder, the average maximum grasp force of gripper with w7-6 and w7-3 were estimated 1297 mN and 1673 mN. On average, the gripper with w7-3 was able to produce a larger grasping force. However, depending on the position of the object and the grasping posture, the gripper with the w7-3 joint also showed slippage at the tip of the fingers at a low grasping force.

VI. Conclusion and Future Work

ARC joint mimicking the tongue-and-groove mechanism and collateral ligaments of a human finger joint was proposed. With elastic ligament and tongue-and-groove mechanism, the ARC joint is compliant, and the torsional stiffness of ARC joint passively increase according to the joint angle. The increment of torsional stiffness can be designed by adjusting the shape of the tongue and groove without additional weight and space. In addition, the ARC joint has a structure that can be completely disassembled and reassembled because it does not use adhesives or knots to fix the ligament, unlike the previous rolling contact joints, and thus is easy to maintain.

One of the applications that utilizes that the torsional stiffness increases as the joint is flexed is grippers because the process of grasping consists of two separate stages; searching and grasping. In the searching stage, the opened gripper (stretched fingers) with lower joint stiffness enables stable contact with objects and environments, and the high joint stiffness of the flexed fingers improves the grasping stability in the grasping stage. The torsional stiffness of six ARC joint was analyzed, and two three-finger grippers with different shapes of ARC joints were designed and fabricated to experimentally demonstrate that the ARC joint increases grasp stability in pinch grasping of small objects.

The tongue-and-groove shape was limited to a triangle, in this study, but an optimal tongue-and-groove shape will depend on the design purpose of the joint, and further studies are required. Because the ARC joint is inspired by the human finger joint, we plan to design a human-hand-size robotic hand by miniaturizing the ARC joint.

References

[1] C. Piazza, G. Grioli, M. Catalano, and A. Bicchi, "A century of robotic hands," *A. Rev. Control, Robot., Auton. Syst.*, vol. 2, pp. 1–32, 2019.

[2] M. Bonilla et al., "Grasping with soft hands," in *Proc. IEEE-RAS Int. Conf. Humanoid Robots*, 2014, pp. 581–587.

[3] M. Manti, T. Hassan, G. Passetti, N. D'Elia, C. Laschi, and M. Cianchetti, "A bioinspired soft robotic gripper for adaptable and effective grasping," *Soft Robot.*, vol. 2, no. 3, pp. 107–116, 2015.

[4] J. Zhou, S. Chen, and Z. Wang, "A soft-robotic gripper with enhanced object adaptation and grasping reliability," *IEEE Robot. Automat. Lett.*, vol. 2, no. 4, pp. 2287–2293, Oct. 2017.

[5] C. B. Teeple, T. N. Koutros, M. A. Graule, and R. J. Wood, "Multi-segment soft robotic fingers enable robust precision grasping," *Int. J. Robot. Res.*, vol. 39, no. 14, pp. 1647–1667, 2020.

[6] Y.-J. Kim, J. Yoon, and Y.-W. Sim, "Fluid lubricated dexterous finger mechanism for human-like impact absorbing capability," *IEEE Robot. Automat. Lett.*, vol. 4, no. 4, pp. 3971–3978, Oct. 2019.

[7] H. Liu, K. Xu, B. Siciliano, and F. Ficuciello, "The mero hand: A mechanically robust anthropomorphic prosthetic hand using novel compliant rolling contact joint," in *Proc. IEEE/ASME Int. Conf. Adv. Intell. Mechatron.*, 2019, pp. 126–132.

[8] C. L. Collins, "Kinematics of robot fingers with circular rolling contact joints," *J. Robot. Syst.*, vol. 20, no. 6, pp. 285–296, 2003.

[9] C. Della Santina, C. Piazza, G. Grioli, M. G. Catalano, and A. Bicchi, "Toward dexterous manipulation with augmented adaptive synergies: The pisa/iit softhand 2," *IEEE Trans. Robot.*, vol. 34, no. 5, pp. 1141–1156, 2018.

[10] Y. Zhu, G. Wei, L. Ren, Z. Luo, and J. Shang, "An anthropomorphic robotic finger with innate human-finger-like biomechanical advantages Part I: Design, ligamentous joint, and extensor mechanism," *IEEE Trans. Robot.*, early access, Sep. 5, 2022, doi: 10.1109/TRO.2022.3200006.

[11] Y. Zhu, G. Wei, L. Ren, Z. Luo, and J. Shang, "An anthropomorphic robotic finger with innate human-finger-like biomechanical advantages Part II: Flexible tendon sheath and grasping demonstration," *IEEE Trans. Robot.*, early access, Sep. 5, 2022, doi: 10.1109/TRO.2022.3200143.

[12] B. M. Hillberry and A. S. Hall Jr., "Rolling contact joint," U.S. Patent 3,932,045, Jan. 1976.

[13] S.-H. Kim, H. In, J.-R. Song, and K.-J. Cho, "Force characteristics of rolling contact joint for compact structure," in *Proc. IEEE 6th Int. Conf. Biomed. Robot. Biomechatron.*, 2016, pp. 1207–1212.

[14] S. W. Hong, J. Yoon, Y.-J. Kim, and H. S. Gong, "Novel implant design of the proximal interphalangeal joint using an optimized rolling contact joint mechanism," *J. Orthopaedic Surg. Res.*, vol. 14, no. 1, pp. 1–13, 2019.

[15] R. Liang, G. Xu, Q. Zhang, K. Jiang, M. Li, and B. He, "Design and characterization of a rolling-contact involute joint and its applications in finger exoskeletons," *Machines*, vol. 10, no. 5, 2022, Art. no. 301.

[16] D. Zhang, Y. Sun, and T. C. Lueth, "Design of a novel tendon-driven manipulator structure based on monolithic compliant rolling-contact joint for minimally invasive surgery," *Int. J. Comput. Assist. Radiol. Surg.*, vol. 16, no. 9, pp. 1615–1625, 2021.

[17] A. Minami, K.-N. An, W. P. Cooney III, R. L. Linscheid, and E. Y. Chao, "Ligament stability of the metacarpophalangeal joint: A biomechanical study," *J. Hand Surg.*, vol. 10, no. 2, pp. 255–260, 1985.

[18] S. Kamnerdnakta, H. E. Huetteman, and K. C. Chung, "Complications of proximal interphalangeal joint injuries: Prevention and treatment," *Hand Clin.*, vol. 34, no. 2, pp. 267–288, 2018.

[19] C. Dumont, G. Albus, D. Kubein-Meesenburg, J. Fanghänel, K. M. Stürmer, and H. Nägerl, "Morphology of the interphalangeal joint surface and its functional relevance," *J. Hand Surg.*, vol. 33, no. 1, pp. 9–18, 2008.